

# MicroRNA-155 controls vincristine sensitivity and predicts superior clinical outcome in diffuse large B-cell lymphoma

Hanne Due,<sup>1</sup> Anna Amanda Schönherz,<sup>1,2</sup> Laura Ryø,<sup>1,3</sup> Maria Nascimento Primo,<sup>3</sup> Ditte Starberg Jespersen,<sup>1</sup> Emil Aagaard Thomsen,<sup>3</sup> Anne Stidholt Roug,<sup>1</sup> Min Xiao,<sup>4</sup> Xiaohong Tan,<sup>4</sup> Yuyang Pang,<sup>4</sup> Ken H. Young,<sup>4</sup> Martin Bøgsted,<sup>1,5,6</sup> Jacob Giehm Mikkelsen,<sup>3</sup> and Karen Dybkær<sup>1,5,6</sup>

<sup>1</sup>Department of Hematology, Aalborg University Hospital, Aalborg, Denmark; <sup>2</sup>Center for Quantitative Genetics and Genomics, Department of Molecular Biology and Genetics, and <sup>3</sup>Department of Biomedicine, Aarhus University, Aarhus, Denmark; <sup>4</sup>The University of Texas MD Anderson Cancer Center, Houston, TX; <sup>5</sup>Clinical Cancer Research Center, Aalborg University Hospital, Aalborg, Denmark; and <sup>6</sup>Department of Clinical Medicine, Aalborg University, Aalborg, Denmark.

## Key Points

- Induced miR-155 expression promotes vincristine sensitivity in DLBCL cell lines.
- High miR-155 expression is associated with superior clinical outcome in patients with DLBCL of the GCB subclass.

A major clinical challenge of diffuse large B-cell lymphoma (DLBCL) is that up to 40% of patients have refractory disease or relapse after initial response to therapy as a result of drug-specific molecular resistance. The purpose of the present study was to investigate microRNA (miRNA) involvement in vincristine resistance in DLBCL, which was pursued by functional *in vitro* analysis in DLBCL cell lines and by outcome analysis of patients with DLBCL treated with rituximab, cyclophosphamide, doxorubicin, vincristine, and prednisone (R-CHOP). Differential miRNA expression analysis identified miR-155 as highly expressed in vincristine-sensitive DLBCL cell lines compared with resistant ones. Ectopic upregulation of miR-155 sensitized germinal-center B-cell-like (GCB)–DLBCL cell lines to vincristine, and consistently, reduction and knockout of miR-155 induced vincristine resistance, documenting that miR-155 functionally induces vincristine sensitivity. Target gene analysis identified miR-155 as inversely correlated with *Wee1*, supporting *Wee1* as a target of miR-155 in DLBCL. Chemical inhibition of *Wee1* sensitized GCB cells to vincristine, suggesting that miR-155 controls vincristine response through *Wee1*. Outcome analysis in clinical cohorts of DLBCL revealed that high miR-155 expression level was significantly associated with superior survival for R-CHOP-treated patients of the GCB subclass, independent of international prognostic index, challenging the commonly accepted perception of miR-155 as an oncomiR. However, miR-155 did not provide prognostic information when analyzing the entire DLBCL cohort or activated B-cell-like classified patients. In conclusion, we experimentally confirmed a direct link between high miR-155 expression and vincristine sensitivity in DLBCL and documented an improved clinical outcome of GCB-classified patients with high miR-155 expression level.

## Introduction

Diffuse large B-cell lymphoma (DLBCL) is the most frequent type of non-Hodgkin's lymphoma, characterized by great heterogeneity regarding clinical presentation, tumor biology, and prognosis.<sup>1</sup> Gene expression profiling (GEP) defines cell-of-origin subtypes reflecting normal B-cell differentiation stages and permits classification of DLBCL into activated B-cell-like (ABC) and germinal-center B-cell-like (GCB), which differ in pathogenic activation mechanisms, genetic aberrations, and clinical outcome.<sup>2,3</sup> Although this classification has expanded our biological understanding of DLBCL, molecular mechanisms related to treatment response and resistance are still not fully understood.

The addition of rituximab (R) to the multiagent chemotherapy regimen cyclophosphamide, doxorubicin, vincristine, and prednisolone (CHOP) has increased DLBCL survival substantially; however, 30% to 40% of patients ultimately die of relapse or refractory disease because of treatment resistance.<sup>4-6</sup> As a consequence, novel treatments and predictive biomarkers are urgently warranted, and equally important, improved biological understanding is required for mechanisms leading to resistance. Several clinical trials have aimed at improving the R-CHOP regimen by dose adjustments, cycles, or add-on drugs, but with limited benefit, emphasizing that increased knowledge of R-CHOP resistance is still highly relevant.<sup>7-9</sup> The antimitotic drug vincristine has been used as anticancer therapy for more than 40 years and is a cornerstone for efficacy of R-CHOP because of its broad cytotoxic effect, limited bone marrow suppression, and high tolerability.<sup>10,11</sup> Despite wide use of vincristine, little is known about determinants of vincristine resistance in treatment of DLBCL, a caveat when attempting to improve clinical outcome.

Recent studies demonstrate that noncoding RNAs, and in particular microRNAs (miRNAs), play important roles in the pathogenesis of DLBCL.<sup>12-14</sup> miRNAs regulate gene expression by targeting mRNA for translational repression or degradation and are involved in cardinal physiologic and pathologic processes.<sup>15</sup> Aberrant miRNA expression is a common feature of malignancies and has been linked to chemotherapy resistance.<sup>16-18</sup> One of the most extensively studied miRNAs in normal B-cell differentiation and hematological cancers is miR-155,<sup>19,20</sup> which acts as an oncomiR in the pathogenesis and aggressiveness of DLBCL.<sup>21</sup> In line, miR-155 levels in patients with ABC are significantly higher compared with those detected in patients classified as having GCB,<sup>19</sup> and transgenic mice overexpressing miR-155 spontaneously develop DLBCL,<sup>22</sup> emphasizing its importance in lymphomagenesis.

Early detection of drug-specific resistance is of pivotal importance to successful cancer therapy, and defining miRNA involvement could provide information on resistance mechanisms of the drug and make miRNAs themselves biomarkers and treatment targets. Because vincristine is a cornerstone in the treatment of DLBCL, we studied the involvement of miRNAs in the response to this antimitotic drug. To pinpoint miRNAs controlling vincristine response, 13 DLBCL cell lines were subjected to systematic dose-response experiments and grouped as resistant, intermediate, or sensitive.<sup>23</sup> Global miRNA expression profiling of these cell lines in untreated condition was performed and miRNAs differentially expressed between vincristine sensitive and resistant cell lines were identified, showing miR-155 to be highly expressed in vincristine-sensitive cells. Hence, experimental manipulations of miR-155 expression using lentiviral gene delivery in DLBCL cells were performed to determine the functional effect of miR-155 in vincristine response, and subsequently a prognostic value of miR-155 was documented in 2 independent R-CHOP-treated DLBCL cohorts.

## Materials and methods

### Cell lines

DLBCL cell lines (supplemental Table 1) were cultured at 37°C in a humidified atmosphere of 95% air and 5% CO<sub>2</sub> with RPMI1640 medium, 10% fetal bovine serum, and 1% penicillin/streptomycin. HEK293T cells were maintained in Dulbecco's modified Eagle medium containing 5% fetal bovine serum and 1% penicillin/streptomycin.

All cell lines were authenticated by DNA barcoding<sup>23</sup> and examined for mycoplasma infection.

### Clinical samples

Diagnostic biopsies from 73 patients with DLBCL (supplemental Table 2) were collected in agreement with the RetroGen research protocol and reviewed and approved by the health ethic committee of the North Denmark Region (approval jr. no. N-20140099), allowing exemption from the Declaration of Helsinki requirement of informed consent according to sections 3 to 5 in the Danish Act on Research Ethics Review of Health Research Projects. Informed consent was waived, as this notifiable database research project did not involve any health risks and, under the given conditions, could not otherwise put a strain on the trial subject. In addition, it would be impossible or disproportionately difficult to obtain informed consent or proxy consent, respectively, because of the use of archival samples and because several patients have died since collection. Of the 73 patients with DLBCL, 69 were treated with standard R-CHOP. In addition, we used Gene Expression Omnibus data (GSE10846<sup>24</sup> and GSE31312<sup>3</sup>).

### Dose-response assays

Vincristine dose-response screens were performed on DLBCL cell lines, as previously described.<sup>23,25</sup> Each cell line was subjected to 18 increasing concentrations for 48 hours, and dose-responses were evaluated using a 3-(4,5 dimethylthiazol-2-yl)-5-(3-carboxymethoxyphenyl)-2-(4-sulfophenyl)-2H-tetrazolium assay.

### RNA extraction

RNA was extracted using a protocol combining TRIzol (Invitrogen) and mirVana miRNA Isolation Kit (Ambion/ThermoFisher Scientific)<sup>26</sup> or a RNAqueous Micro scale RNA Isolation kit (<500 000 cells; ThermoFisher Scientific). RNA integrity and concentration were determined using an Agilent 2100 Bioanalyzer and NanoDrop ND-1000 spectrophotometer, respectively.

### Microarray profiling

miRNA expression profiling was performed using GeneChip miRNA 1.0.2 arrays (Affymetrix), as previously described,<sup>17</sup> and CEL files are deposited at Gene Expression Omnibus (GSE72648). GEP of clinical samples and transduced SU-DHL-5 cells was performed using Affymetrix GeneChip HG-U133 Plus2.0 arrays. CEL files were generated using the Affymetrix Gene-Chip Command Console Software and deposited at Gene Expression Omnibus (GSE109027). Data comply with Minimum Information About a Microarray Experiment requirements.

### Reverse transcription quantitative polymerase chain reaction

miR-155 expression was determined by TaqMan miRNA reverse transcription quantitative polymerase chain reaction (RT-qPCR; Thermo Fisher Scientific). Two independent cDNA syntheses were conducted and pooled before amplification qPCR analysis (hsa-miR-155 [002623], RNU6B [001093], RNU24 [001001]). Each sample was analyzed in triplicate, using Mx3000P (Stratagene/Agilent Technologies). miRNA expression was normalized to RNU6B and RNU24 and log<sub>2</sub> transformed.

### Plasmid construction

A lentiviral vector containing multiple cloning sites for insertion of PCR-amplified miRNA sequences was generated.<sup>27,28</sup> The sequence

encoding pri-miR-155 was amplified from HeLa cells, using primers 5'-AAAGCGGCCGCCATCTTTAATTGCCAATTTCTCTACC-3' and 5'-AAAGCGGCCGCGTTAAGGTTGAACATCCCAGT-GACC-3'. Fragments were *NotI*-digested and inserted into *Bsp120I* digested plasmid from corynebacterium callunae (pCCL) with a multiple cloning site (MCS) immediately downstream of the H1 promoter (H1) and phosphoglycerate kinase promoter (PGK) controlling enhanced green fluorescent protein (eGFP) (pCCL/H1-MCS-PGK-eGFP). For miR-155 inhibition, a Tough Decoy (TuD)-expressing construct with high miRNA-suppressive capacity was generated by a 2-step cloning strategy.<sup>29,30</sup> DNA sequences containing inhibitor sequence flanked by *NheI/Ascl* sites were synthesized and cloned into pUC57 by GeneScript. Inhibitor sequences were cleaved from pUC57 and cloned into *AvrIII/Ascl*-digested pCCL/PKG-eGFP.H1-MCS. Sequences including TuD were PCR-amplified from lentiviral vectors encoding H1 driven inhibitor, using 5'-AAAAGGTACCGTATGAG-ACCACCCTAGCCC-3' and 5'-AAAAGGTACCCAGAGAGACC-CAGTACAAGC-3'. *KpnI*-digested PCR products were cloned into *KpnI*-digested pCCL/PKG-eGFP.

To test functionality, sense and antisense oligonucleotides harboring miR-155 target sequence were annealed and cloned into *NotI/XhoI*-digested psiCHECK-2 vector (Promega).<sup>29</sup> Co-transfections of HEK293T cells were performed with 7 ng pCCL/U1-miRNA, PGK-eGFP, 14ng psiCHECK-miRtarget, and 80 ng pCCL/PKG-eGFP-TuD, using X-tremeGENE 9 (Roche). Renilla and Firefly luciferase expression levels were measured 48 hours posttransfection, using Dual-Glo Luciferase Reporter Assay System (Promega). Renilla luciferase activity was normalized to Firefly and presented relative to negative control (pCCL/PKG-eGFP).

All plasmids were verified by sequencing (GATC; Konstanz, Germany).

### Lentivirus production and transduction

To generate lentiviral vectors,  $1 \times 10^7$  HEK293T cells were seeded in 25 mL Dulbecco's modified Eagle medium. Twenty-four hours after seeding, cells were transfected with 9.07  $\mu$ g pMD.2G, 7.26  $\mu$ g pRSV-Rev, 31.46  $\mu$ g pMDlg/p-RRE, and 31.46  $\mu$ g lentiviral transfer vector. Both 48 and 72 hours posttransfection, viral supernatant was harvested, filtered (0.45  $\mu$ m), and ultracentrifuged. Virus yield was determined by measurements of p24 capsid protein, using p24 Antigen ELISA Kit (XpressBio). DLBCL cells were seeded at 300 000 cells/mL in 1 mL standard RPMI and transduced with virus corresponding to 85 ng p24. DLBCL cell lines SU-DHL-5, OCI-Ly7, NU-DHL-1, and RIVA were selected on the basis of ABC/GCB classification, resistance/sensitivity to vincristine, and lentiviral transducibility.<sup>27</sup> RT-qPCR was used to confirm changes in miR-155 expression.

### CRISPR-Cas9 knockout

Single guide RNA (sgRNA) was designed to target the functional part of *MIR155HG* (supplemental Figure 1). Sense and antisense oligonucleotides encoding the sgRNA were annealed and cloned into pLV/CRISPR-v2, using *BsmBI* site.<sup>31</sup> OCI-Ly7 was transduced with LV/CRISPR-sgRNA-miR-155 or LV/CRISPR-sgRNA-control, the latter without target in the human genome (5'-ACGGAGGCTAAGC-GTCGCAA-3') and subjected to puromycin selection (0.5  $\mu$ g/mL). After 2 weeks, gDNA was extracted using standard NaCl/EtOH precipitation protocol, and gDNA encompassing the Cas9 cut sites was amplified using 5'-AACTCCGAAGAGCGGTT-3' and 5'-GGTTGA-ACATCCCAGTGACC-3'. Indel frequencies were determined by sequence-based Tracking of Indels by Decomposition analysis.<sup>32</sup>

miR-155 knockout clones from single-cell expansion were generated by seeding 96-well plates at concentrations of 0.5 cell/well in 50  $\mu$ L standard RPMI, 100  $\mu$ L conditioned medium, and 50  $\mu$ L RPMI containing 55% fetal bovine serum and 3% penicillin/streptomycin. Tracking of Indels by Decomposition analysis and RT-qPCR was performed in individual clones.

### Dose-response screen of transduced cells

Transduced cells and miR-155 knockout clones were seeded at  $3 \times 10^5$  cells/mL in 1 mL standard RPMI. Cells were exposed to vincristine for 48 hours, and viable cells were counted using trypan blue exclusion. Transduced cells were treated with 2 concentrations of vincristine (0.0005-0.001  $\mu$ g/mL), whereas miR-155 knockout cells were exposed to 0.0005, 0.001, and 0.0015  $\mu$ g/mL. Transductions and functional assays were performed in triplicate in 2 independent assays.

### Western blot

Cell lysates were prepared using RIPA Lysis Buffer supplemented with complete miniprotease inhibitors, and protein concentration was determined using BCA Pierce (Thermo Fisher Scientific). Western blotting analysis was performed following standard Bio-Rad procedures loading 20  $\mu$ g total protein. Antibodies used were  $\beta$ -actin (1:10 000, Abcam, ab6276), Wee1 (1:1,000, Santa Cruz Biotechnology, sc-5285), Ship-1 (1:1000, Santa Cruz Biotechnology, sc-8425), and rabbit-anti-mouse IgG (1:10 000, Abcam, ab6728).

### Double drug analysis

Wee1 inhibitor MK-1775 (Selleck chemical) was dissolved in dimethyl sulfoxide. OCI-Ly7 cells were seeded in 96-well plates at a density of  $0.25 \times 10^6$  cells/mL, 24 hours before drug was added. Cells were exposed to 0.0015  $\mu$ g/mL vincristine, 400 nM MK-1775, or 0.0015  $\mu$ g/mL vincristine and 400 nM MK-1775 for 48 hours, and metabolically active cells were determined by 3-(4,5-dimethylthiazol-2-yl)-5-(3-carboxymethoxyphenyl)-2-(4-sulfophenyl)-2H-tetrazolium-containing CellTiter 96 Reagent at a concentration of 20% of pre-additional well content. Absorbance was measured at 492 nm (BMG, LABTECH).

### Statistical analysis

Statistical analyses were performed with R (v.3.3.3).<sup>33</sup> Array-based miRNA and gene expression data were cohort-wise background corrected and normalized at the probe and gene level, applying a Robust Multichip Average approach,<sup>34</sup> respectively.

Differential miRNA expression analysis was performed using the *limma* Bioconductor package (v.3.26.9),<sup>35</sup> setting  $P < .05$  and  $FC > |2|$  as the significance threshold.

To increase statistical power, external R-CHOP restricted cohorts<sup>3,24</sup> were combined into a meta-cohort. The meta-cohort was batch corrected using ComBat implemented in the *sva* Bioconductor package (v.3.18.0),<sup>36,37</sup> and miR-155 expression was quantified through the *MIR155HG* probe set 229437\_at included in HG-U133 Plus2.0 GeneChip. Validity of array-based quantification was confirmed through correlation analysis, with RT-qPCR quantified miR-155 expression in the in-house cohort.

Confounding effects of ABC/GCB subclasses and Cheson response evaluation on miR-155 expression were investigated through simple

linear regression analysis. Survival analyses were performed using Kaplan-Meier and log-rank test statistics for progression-free survival (PFS) and overall survival (OS). Furthermore, simple and multiple Cox proportional hazards regression analyses were conducted using an additive model with international prognostic index, ABC/GCB, and miR-155 expression (dichotomized by median split into low and high or as a continuous variable) as independent confounders. Linear regression and survival analyses were conducted for all patients with DLBCL and restricted to ABC and GCB classified patients, respectively.

Gene set enrichment analysis (GSEA) was performed for transduced cells (miR-155 vs control and TuD-155 vs control), using the GSEA desktop application (v.3.0)<sup>38</sup> with preranked gene lists, 2000 permutations of gene set randomization, and default settings otherwise. GSEA was restricted to gene sets included in the *Hallmark* collection from the Molecular Signatures Database (v.6.0),<sup>38,39</sup> excluding sets with fewer than 15 or more than 500 genes. Gene sets with normalized  $P \leq .05$  and FDR  $q \leq 0.25$  were considered significantly enriched.

If not mentioned otherwise, 2-sided Student *t* tests were performed to evaluate statistical significance, and significance thresholds were set to 0.05.

## Results

### Identification of vincristine response-specific miRNAs

DLBCL cell lines subjected to vincristine dose-response screens were ranked according to their sensitivity, using area under the dose-response curve, and trichotomized into groups of sensitive, intermediate, and resistant cells (supplemental Table 1).<sup>23,25</sup> To identify miRNAs associated with vincristine response, global miRNA profiling was conducted for each cell line in untreated condition, and subsequent differential miRNA expression analysis between vincristine-sensitive and vincristine-resistant cell lines identified 15 differentially expressed miRNAs (supplemental Table 3). Low miR-155 expression displayed the strongest association to vincristine resistance and was selected for further analyses (supplemental Figure 2). Of notice, miR-155 was the top candidate irrespective of split strategy used to categorize cell lines as sensitive and resistant (4 sensitive, 5 intermediate, and 4 resistant; 6 sensitive and 7 resistant; data not shown).

### Downregulation of miR-155 promotes vincristine resistance

To substantiate involvement of miR-155 in vincristine response, lentiviral vectors encoding pri-miR-155 or TuD-155 for stable up- and downregulation, respectively, were designed (Figure 1A).

Two GCB-DLBCL cell lines, SU-DHL-5 and OCI-Ly7, that are intrinsically sensitive and resistant, respectively, to vincristine with high and low levels of endogenous miR-155 (supplemental Table 1) were transduced. Forty-eight hours posttransduction, the expression level of miR-155 was significantly increased by lentiviral vectors encoding pri-miR-155 and reduced by TuD-155 (Figure 1B-E). Ectopic expression of miR-155 did not have toxic effects because total cell number was unchanged (supplemental Figure 3). Moreover, GSEA conducted for transcriptional profiles of transduced SU-DHL-5 cells revealed that top enriched gene sets detected in miR-155 overexpressing cells compared with controls were

associated with G2/M checkpoints and mitotic spindle assembly. Consistently, those gene sets were enriched in control samples when compared with cells with miR-155 knock-down (supplemental Tables 4 and 5; supplemental Figure 4). Based on the antimetabolic effect of vincristine, those results suggest that miR-155 and vincristine affect comparable biological processes.

Induction of miR-155 significantly increased vincristine sensitivity in both GCB cell lines, and decreased miR-155 expression consistently caused vincristine resistance in intrinsic vincristine-sensitive SU-DHL-5 cells, whereas no change in response was observed in the vincristine-resistant cell line OCI-Ly7 (Figure 1Bii-Eii). Because downregulation of miR-155 did not affect vincristine response in OCI-Ly7, 2 miR-155 knockout clones were generated (supplemental Figure 5; Figure 2B). As a result of miR-155 depletion, cell viability decreased, whereas no difference between vector control and the parental wild-type counterpart was observed (Figure 2A). Furthermore, miR-155 knockout increased vincristine resistance over a range of concentrations (Figure 2C), indicating that miR-155 functionally affected vincristine response in DLBCL cells of the GCB subclass.

In addition, ABC cell lines RIVA and NU-DHL-1, characterized by intrinsically intermediate response to vincristine and comparably high endogenous expression of miR-155 (supplemental Table 1), were similarly analyzed. Applying the TuD model system decreased miR-155 expression in RIVA cells; however, it did not cause unambiguous effect on vincristine sensitivity (supplemental Figure 6BI-BII). Although functionality of the model systems was confirmed (supplemental Figure 7),<sup>28</sup> transduction with LV/miR-155 in RIVA and LV/TuD-155 in NU-DHL-1 did not generate significant changes in intracellular levels of miR-155, and consequently, vincristine dose-response analysis was not performed (supplemental Figure 6AI,DI). Overexpression of miR-155 in NU-DHL-1 cells did not affect vincristine response either (supplemental Figure 6CI-CII), indicating that miR-155 does not play a pivotal role in vincristine response in ABC cells as opposed to GCB cells.

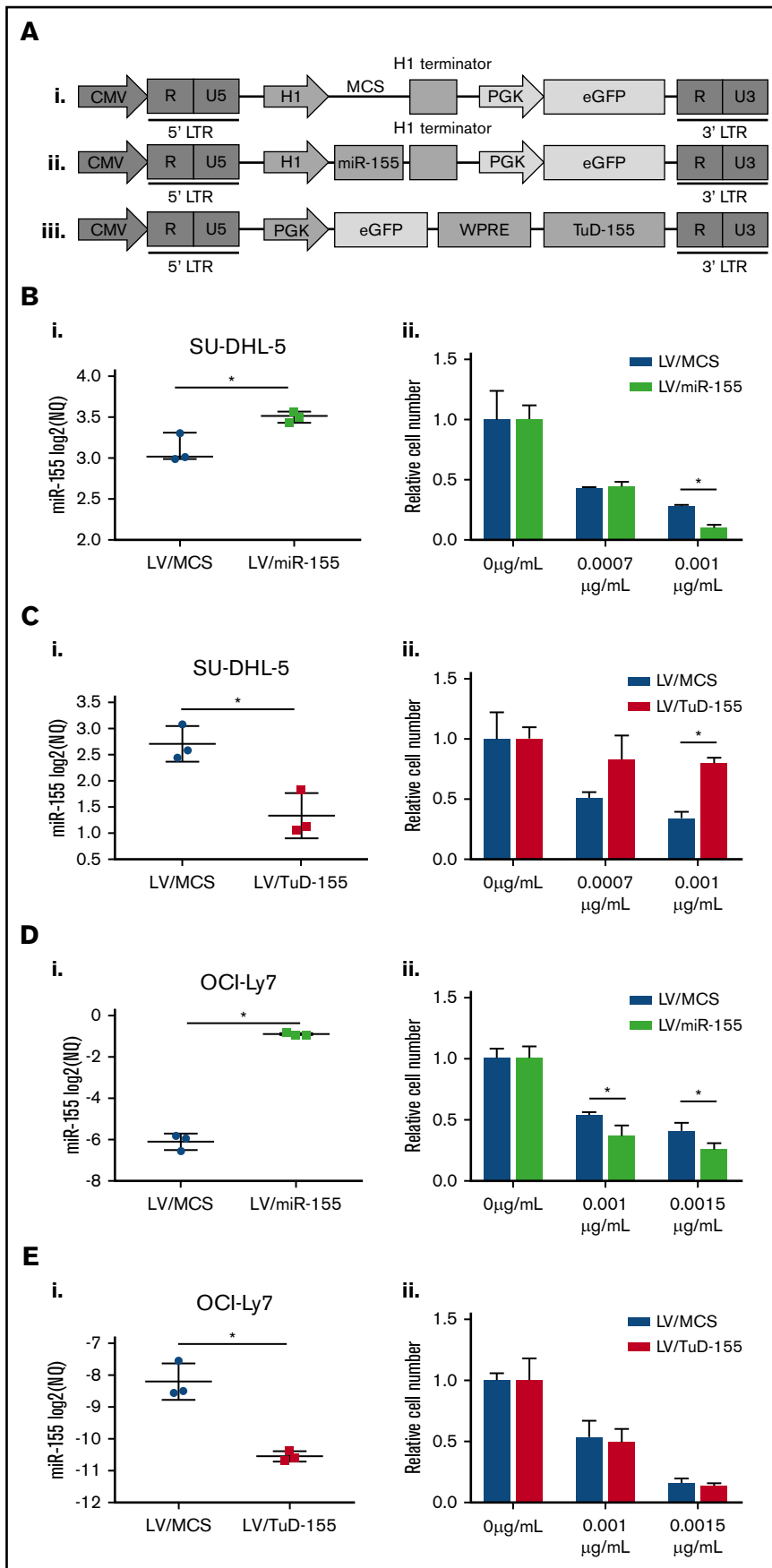
### The cell-cycle checkpoint gene *WEE1* is a direct target of miR-155

To identify target genes of miR-155 with an effect on vincristine response, transcriptional profiles of ectopic miR-155 expressing SU-DHL-5 cells were analyzed. On the basis of the antimetabolic effect of vincristine, resistance mechanisms could be related to cell cycle processes, and thus negatively correlated genes associated with gene ontologies of cell cycle processes were selected ( $n = 64$ ; supplemental Table 6).

To investigate whether selected genes were potential miR-155 targets, miR-155-mRNA interaction was investigated using well-documented miRNA prediction algorithms (TargetScan, miRDB, microT-CDC, and microRNA.org) and TarBase, a database of experimentally validated miRNA-mRNA interactions. Only 1 gene, *WEE1*, was predicted as a putative miR-155 target by all algorithms, and was found as experimentally verified in TarBase. Notably, the miR-155 binding site of *WEE1* is actively recognized by miR-155 in luciferase-based reporter assays,<sup>40,41</sup> and in agreement, induced protein level of Wee1 was observed in miR-155 knockout clones (Figure 2D-E). *WEE1* encodes a kinase controlling G2/M phase by inhibitory phosphorylation of Cdk1, through which Wee1 also affects sensitivity to antimicrotubule drugs.<sup>42</sup> In accordance,

**Figure 1. Changes in miR-155 expression in GCB-DLBCL cell lines affect vincristine response.**

(A) Schematic overview of lentiviral vector plasmids used as control (i), for expression of miR-155 (ii) and TuD-155 (iii) inhibitor in fusion with eGFP. (B-E) Up- and downregulation of miR-155 was detected by RT-qPCR in (Bi,Ci) SU-DHL-5 and (Di,Ei) OCI-Ly7 cells and followed by vincristine dose-response analysis. (Bii,Cii,Dii,Eii) Drug response is illustrated as percentage of living cells related to the no-drug treated condition. CMV, cytomegalovirus promoter; LTR, long terminal repeat; NQ, normalized quantity; PGK, phosphoglycerate kinase promoter; WPRE, woodchuck hepatitis virus posttranscriptional regulatory element.



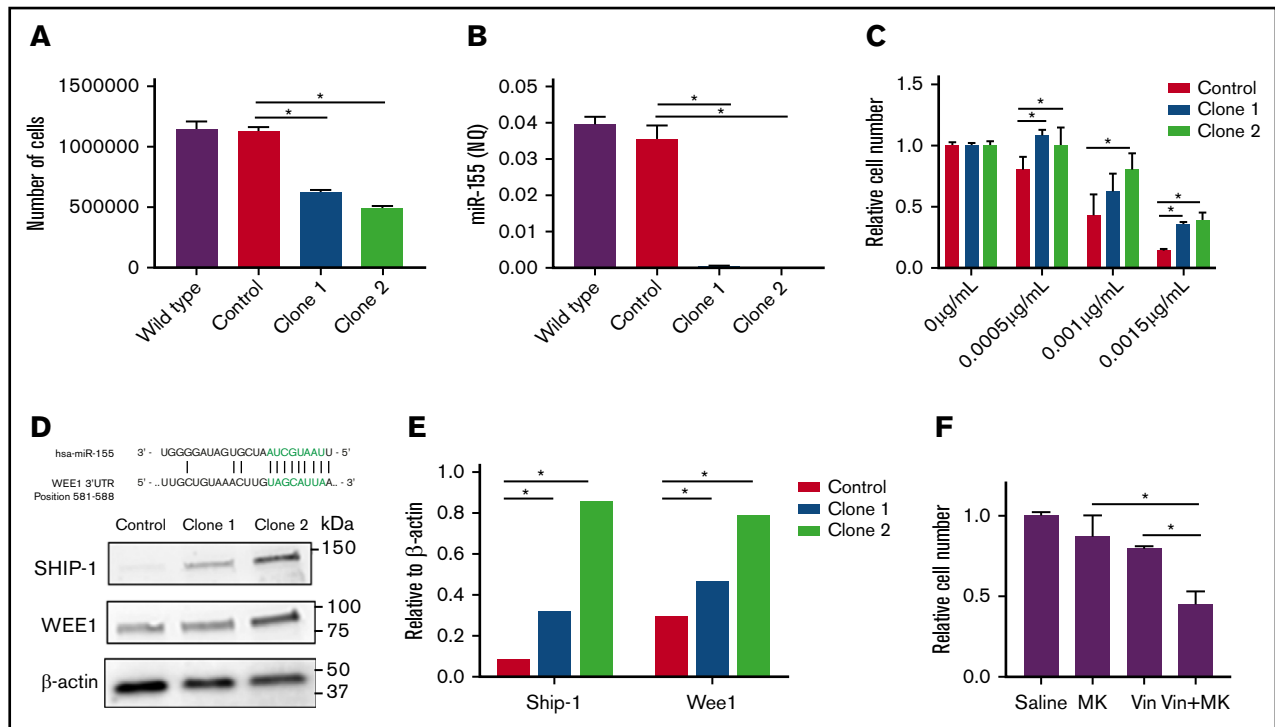


**Figure 2. miR-155 knockout experiments.** Two independent miR-155 knockout clones were generated in OCI-Ly7 cells by the CRISPR-Cas9 technology. Wild-type accounts for untransduced OCI-Ly7 cells, whereas control is an OCI-Ly7 population subjected to a sgRNA not targeting the human genome. (A) Cell proliferation was determined by the trypan blue exclusion method after 48 hours of growth in wild-type, control cells, and miR-155 knockout clones. (B) miR-155 expression detected by RT-qPCR. (C) Vincristine dose-response analysis using 0.0005 μg/mL, 0.001 μg/mL, and 0.0015 μg/mL. Drug response is illustrated as percentage of living cells related to the no-drug condition. (D) Detection of Wee1 protein by western blotting. β-actin was used as loading control and Ship-1, a validated target of miR-155,<sup>53</sup> as positive control. (E) Quantification of western blot bands. Ship-1 and Wee1 levels are depicted as relative to β-actin levels. (F) Chemical inhibition of Wee1 by MK-1775. Wild-type OCI-Ly7 cells were exposed to saline, 400 nM MK-1775, 0.0015 μg/mL vincristine or 400 nM MK-1775 and 0.0015 μg/mL vincristine for 48 hours, and the number of metabolically cells were determined by 3-(4,5 dimethylthiazol-2-yl)-5-(3-carboxymethoxyphenyl)-2-(4-sulfophenyl)-2H-tetrazolium assay. Drug response is presented as the number of cells relative to the no-drug condition. MK, MK-1775; Vin, vincristine.

chemical inhibition of Wee1 in wild-type OCI-Ly7 cells decreased the number of living cells and enhanced killing when given in combination with vincristine (Figure 2F).

### Prognostic effect of miR-155 expression in GCB-DLBCL

The relationship between miR-155 expression and ABC/GCB subclasses was examined in the in-house cohort, for which miR-155 expression was assayed by RT-qPCR. Higher expression of miR-155 was observed in the ABC subclass (supplemental Figure 8), in accordance with previous observations.<sup>19</sup>

To investigate the prognostic value of miR-155, dichotomized miR-155 expression was analyzed for association with OS and PFS in R-CHOP-treated patients. Because miR-155 is differentially expressed between patients with ABC and GCB-DLBCL, which display different pathogenesis and prognosis, survival analysis was performed both overall and according to ABC and GCB subclasses. A tendency for association between miR-155 and OS and PFS was observed in the entire DLBCL cohort and for GCB-classified patients, with low miR-155 expression characterizing poor outcome (Figure 3; supplemental Figure 9).

To verify this trend, we investigated the prognostic value in an independent meta-cohort of 701 patients with DLBCL, in which

miR-155 expression was quantified through the precursor *MIR155HG*. In the in-house cohort, mature miR-155 expression measured by RT-qPCR was highly correlated to its precursor measured by microarray (supplemental Figure 10), supporting array-based miR-155 expression assessment. Analysis of these data revealed differential expression of miR-155 between ABC and GCB-DLBCL (supplemental Figure 8), consistent with the in-house cohort.

When evaluating the prognostic effect of miR-155 expression, prognostic stratification was confirmed within the GCB subclass, with significantly shorter OS and PFS of patients with low levels of miR-155 (Figure 4). However, miR-155 expression did not provide prognostic information within the ABC subclass or the entire cohort. These observations were supported by simple Cox proportional hazards regression analysis (Table 1), and are in accordance with the in-house cohort.

In addition, multiple Cox proportional hazards regression analysis was conducted to test the prognostic value of miR-155 when combined with other prognostic tools of DLBCL. For multiple Cox regression analysis, independent variables were only included in the model if significant results were obtained when performing simple Cox regression analyses. The analysis revealed that the prognostic value of miR-155 was independent of the well-established international prognostic index in the GCB subclass, irrespective of

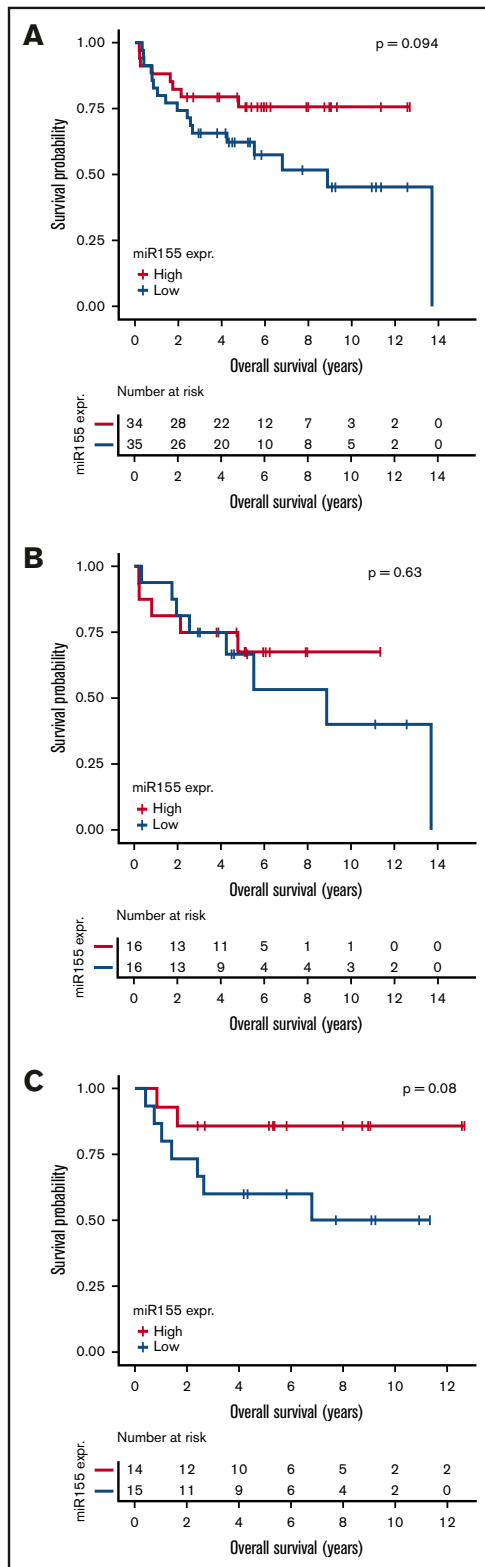


**Figure 3. Analysis of prognostic effect of miR-155 expression.** Kaplan-Meier plots depicting OS of R-CHOP-treated patients with DLBCL in the in-house cohort. The analysis was conducted for all patients with DLBCL (A), ABC-classified patients (B), and GCB-classified patients (C). For each cohort, patients were dichotomized by median split of miR-155 expression.

dichotomized or continuous miR-155 expression (Table 1; supplemental Table 7). Thus, miR-155 identifies a subgroup with inferior prognosis among GCB-classified patients. In accordance, patients with stable or progressive disease at time of response evaluation<sup>43</sup> display lower levels of miR-155 than patients in complete remission (supplemental Figure 11), supporting the association between low miR-155 expression and vincristine resistance.

## Discussion

In a 2-step strategy, we defined miRNA involvement in vincristine resistance in DLBCL, first by elucidating the biological role of miRNAs in vincristine response by functional analysis and second by evaluating the biomarker potential in 2 independent R-CHOP-treated DLBCL cohorts. Identification of vincristine response-specific miRNAs documented miR-155 as highly expressed in vincristine-sensitive DLBCL cell lines, and functional validation confirmed a direct link between miR-155 expression and vincristine response in DLBCL cells. To compensate for cell line-specific biological effects, analyses were performed in 2 ABC and GCB-DLBCL cell lines, strengthening the biological interpretation. Induction of miR-155 increased vincristine sensitivity in GCB cells, with the strongest phenotype obtained in vincristine-resistant OCI-Ly7. The endogenous level of miR-155 is relatively low in OCI-Ly7, supporting significantly increased effect on vincristine response on induction. Only a complete knockout generated by indel introduction induced clear cellular resistance in OCI-Ly7, showing that TuD-155-directed reduction of already low miR-155 levels was not sufficient to cause phenotypic alterations. When applying similar approaches in ABC cells, no unambiguous association between miR-155 and vincristine response was observed. However, as a result of high endogenous miR-155 expression in ABC cells, it may be challenging to further increase miR-155 levels. In GCB cells, in contrast, lentiviral intervention altered the intracellular level of miR-155 independent of endogenous levels, suggesting a more stringent and complex regulation of miR-155 in ABC-DLBCL. Of notice, miR-155 is regulated by a feedback loop through NF- $\kappa$ B signaling, a pathway reported to be constitutively active in ABC-DLBCL.<sup>44,45</sup>

GSEA revealed that ectopic expression of miR-155 affected G2/M checkpoints and genes involved in mitotic spindle assembly. In accordance, the cell-cycle checkpoint gene *WEE1* was inversely correlated with miR-155 in exogenously modified GCB-DLBCL cells, and in addition, induced levels of Wee1 protein were observed in miR-155 knockout clones. Although Wee1 is an experimentally verified target of miR-155,<sup>41</sup> it has not previously been validated in DLBCL cells, which is of great importance, as affected targets vary depending on the cell type in which the miRNA is expressed.<sup>46</sup>

A study by Visconti et al.<sup>42</sup> reported that the Fcp1-Wee1-Cdk1 axis controls spindle assembly checkpoints (SAC), which ensures proper chromosome segregation by delaying mitosis exit until mitotic spindle assembly.<sup>47</sup> Antimicrotubule drugs, including vincristine, impede mitotic spindle assembly by targeting microtubules, leading to the activation of SAC and extension of mitosis, which promotes apoptosis.<sup>47,48</sup> Resistance to these types of drugs has been related to the ability of cancer cells to slip through the SAC and exit mitosis prematurely, and thereby resist killing.<sup>48,49</sup> Activation of Wee1 stimulates SAC slippage,<sup>42</sup> suggesting that increased vincristine resistance mediated by

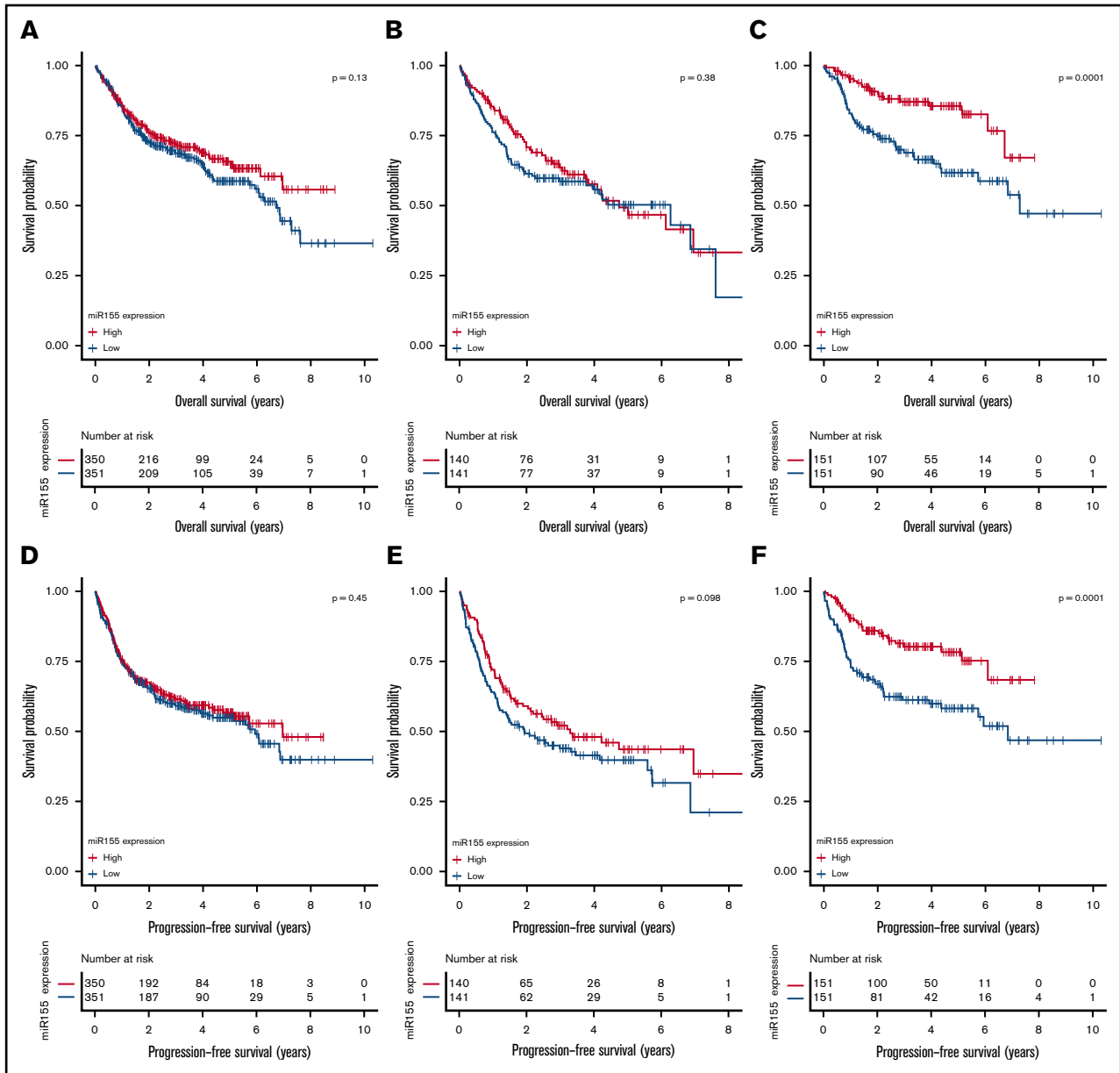


**Figure 4. Analysis of association between OS and PFS and miR-155 expression.** Kaplan-Meier plot depicting OS (A-C) and PFS (D-F) of R-CHOP-treated patients with DLBCL in the meta-cohort, consisting of R-CHOP–restricted Lymphoma/Leukemia Molecular Profiling Project and International DLBCL Rituximab-CHOP Consortium MD Anderson Project data. Before analysis, data were ComBat normalized to compensate for study-wise batch effect. Analyses were conducted for all patients with DLBCL (A,D), ABC-classified patients (B,E), and GCB-classified patients (C,F). For each cohort, patients were dichotomized by median split of *MIR155HG* expression.

miR-155 knockout could occur through upregulation of Wee1 and increased Wee1 signaling. However, it is important to emphasize that this study only addresses miR-155 signaling through Wee1. miR-155 could mediate vincristine resistance by regulating other targets as well, yet comprehensive target gene analysis was not the focus in this study.

Genetic and chemical inhibition of Wee1 strengthens the SAC, prolongs mitosis, and enhances killing of vincristine-treated acute lymphoblastic leukemia cells.<sup>42,50</sup> In agreement, MK-1775, a chemical inhibitor of Wee1, boosted the effect of vincristine in GCB-DLBCL cells in this study. Interestingly, MK-1775 potentiated the cytotoxic

effect of doxorubicin, another vital component of R-CHOP,<sup>51</sup> supporting combination therapy of R-CHOP and MK-1775 in relapsed or refractory DLBCL.

miR-155 is involved in numerous processes that could affect drug response, including MAPK, PI3K/AKT, and RhoA signaling.<sup>52-55</sup> In line, decreased miR-155 expression in epidermoid carcinoma cells increased cisplatin resistance by increasing the amount of Wee1 protein,<sup>56</sup> similar to the mechanism of miR-155-induced vincristine resistance reported in this study. Furthermore, suppression of miR-155 was found to reverse doxorubicin resistance in lung cancer cells, whereas it did not affect the response in DLBCL cells, highlighting



**Table 1. *MIR155HG* expression is an IPI-independent prognostic marker for R-CHOP-treated patients with GCB-DLBCL**

	n	no.	Simple			Multiple		
			HR	95% CI	P	HR	95% CI	P
<b>All DLBCL</b>								
miR-155								
Low	293	90	1			—		
High	293	107	1.17	0.88-1.54	.28	—	—	—
IPI								
0-1	71	6	1			1		
2-3	314	84	3.76	1.64-8.61	.0017	3.42	1.49-7.84	.0038
4-5	201	106	9.61	4.22-21.88	7.19e-08	8.29	3.62-18.98	5.73e-07
Subclass								
ABC	242	105	1			1		
GCB	248	58	0.45	0.33-0.62	1.09e-06	0.55	0.40-0.76	.00032
UC	96	34	0.73	0.50-1.08	.11	0.71	0.48-1.05	.089
<b>ABC-DLBCL</b>								
miR-155								
Low	121	57	1			—		
High	121	48	0.78	0.53-1.14	.20	—	—	—
IPI								
0-1	15	2	1			—		
2-3	125	38	3.57	0.86-14.89	.080	—	—	—
4-5	102	65	10.37	2.51-42.87	.0012	—	—	—
<b>GCB-DLBCL</b>								
miR-155								
Low	124	41	1			1		
High	124	17	0.40	0.23-0.71	.0017	0.46	0.26-0.81	.0071
IPI								
0-1	48	2	1			1		
2-3	140	32	6.22	1.49-25.97	.012	5.91	1.42-24.69	.015
4-5	60	24	12.53	2.96-53.06	.0006	11.10	2.61-47.15	.0011

Array-based miR-155 expression and outcome were analyzed by simple and multiple Cox proportional hazards regression analyses for OS. IPI (international prognostic index) score information was not available for all patients, thus cohort sizes are reduced in this setting (115 samples were removed). *MIR155HG* expression was dichotomized by median split in each of the individual cohorts: all DLBCL patients, ABC-classified patients, and GCB-classified patients.

—, value not available because variables were only included in multiple Cox proportional hazards regression analysis if significant results were obtained in simple Cox proportional hazards regression analysis; CI, 95% lower and upper confidence intervals; HR, hazard ratio; n, number of samples; no., number of events.

the tissue-specific effect of a particular miRNA.<sup>13,57</sup> Whether miR-155 has an effect on other compounds of R-CHOP is unknown. However, rituximab exerts its action through CD20, whereas cyclophosphamide has alkylating properties and furthermore induces cytokine release, leading to antibody-mediated elimination,<sup>58</sup> all of which are mechanisms differing from those of vincristine. Thus, miR-155 does most likely not affect rituximab and cyclophosphamide response through Wee1, but has the potential through other targets.

To evaluate the prognostic effect of miR-155, expression levels were analyzed for association with clinical outcome. It is noteworthy that the clinical outcome is a result of the entire R-CHOP regimen, and therefore, we investigated the prognostic potential of miR-155 regardless of its association to vincristine response. Investigation of the meta-cohort demonstrated decreased OS and PFS for patients with GCB-DLBCL with low *MIR155HG* expression.

Notably, miR-155 identifies a subgroup of GCB-DLBCL with inferior clinical outcome comparable to ABC-classified patients. The beneficial effect of miR-155 on clinical outcome was a surprising observation when considering the commonly accepted perception of miR-155 as an oncomiR, yet documenting that the effect of a particular miRNA is dependent on the cell type in which it is expressed.

When examining the association between miR-155 and the ABC/GCB subclasses, it was confirmed that miR-155 is more expressed in ABC-DLBCL,<sup>19</sup> which is in accordance with the role of miR-155 as an oncomiR, as ABC-classified patients have a dismal prognosis. Furthermore, clinical analysis revealed that miR-155 only displayed prognostic value within the GCB subclass, highlighting the molecular heterogeneity between the 2 molecular subclasses of DLBCL. These findings, in combination with the different functional effect of miR-155 on vincristine response in ABC and

GCB cells, suggest that miR-155 affects different targets, depending on the cell of origin.

Contradictory to the beneficial effect of miR-155 observed in this study, Iqbal et al<sup>13</sup> reported high miR-155 expression to be associated with R-CHOP treatment failure in DLBCL. However, unlike the current study, patients with DLBCL were divided according to survival risk and not miR-155 expression, and furthermore, without subtype-specific focus. In addition, by dichotomizing patients with DLBCL on miR-155 expression, Zhong et al<sup>59</sup> documented inferior prognosis of patients with DLBCL with high miR-155 levels, whereas no prognostic stratification was observed in the study of Go et al.<sup>60</sup> Yet, to the best of our knowledge, this is the first prognostic evaluation of miR-155 with a DLBCL subtype-specific focus, thereby taking the different pathogenesis of the molecular subclasses into consideration.

In conclusion, experimentally, we confirm a direct functional link between miR-155 expression and vincristine response in DLBCL. This role is supported by prognostic evaluation in 2 independent DLBCL cohorts treated with R-CHOP, documenting a significantly improved clinical outcome of GCB-classified patients with high miR-155 expression. The data suggest that the role of miR-155 on vincristine response is important enough to affect OS and PFS of patients with GCB-DLBCL treated with R-CHOP.

## References

1. Nogai H, Dörken B, Lenz G. Pathogenesis of non-Hodgkin's lymphoma. *J Clin Oncol*. 2011;29(14):1803-1811.
2. Alizadeh AA, Eisen MB, Davis RE, et al. Distinct types of diffuse large B-cell lymphoma identified by gene expression profiling. *Nature*. 2000;403(6769):503-511.
3. Visco C, Li Y, Xu-Monette ZY, et al. Comprehensive gene expression profiling and immunohistochemical studies support application of immunophenotypic algorithm for molecular subtype classification in diffuse large B-cell lymphoma: a report from the International DLBCL Rituximab-CHOP Consortium Program Study. *Leukemia*. 2012;26(9):2103-2113.
4. Coiffier B, Lepage E, Briere J, et al. CHOP chemotherapy plus rituximab compared with CHOP alone in elderly patients with diffuse large-B-cell lymphoma. *N Engl J Med*. 2002;346(4):235-242.
5. Sehn LH, Donaldson J, Chhanabhai M, et al. Introduction of combined CHOP plus rituximab therapy dramatically improved outcome of diffuse large B-cell lymphoma in British Columbia. *J Clin Oncol*. 2005;23(22):5027-5033.
6. Vaidya R, Witzig TE. Prognostic factors for diffuse large B-cell lymphoma in the R(X)CHOP era. *Ann Oncol*. 2014;25(11):2124-2133.
7. Jaeger U, Trneny M, Melzer H, et al; AGMT-NHL13 Investigators. Rituximab maintenance for patients with aggressive B-cell lymphoma in first remission: results of the randomized NHL13 trial. *Haematologica*. 2015;100(7):955-963.
8. Seymour JF, Pfreundschuh M, Trnĕný M, et al; MAIN Study Investigators. R-CHOP with or without bevacizumab in patients with previously untreated diffuse large B-cell lymphoma: final MAIN study outcomes. *Haematologica*. 2014;99(8):1343-1349.
9. Leonard JP, Kolibaba KS, Reeves JA, et al. Randomized phase II study of R-CHOP with or without bortezomib in previously untreated patients with non-germinal center B-cell-like diffuse large B-cell lymphoma. *J Clin Oncol*. 2017;35(31):3538-3546.
10. Gidding CE, Kellie SJ, Kamps WA, de Graaf SS. Vincristine revisited. *Crit Rev Oncol Hematol*. 1999;29(3):267-287.
11. Wilson WH. Treatment strategies for aggressive lymphomas: what works? *Hematology (Am Soc Hematol Educ Program)*. 2013;2013(1):584-590.
12. Verma A, Jiang Y, Du W, Fairchild L, Melnick A, Elemento O. Transcriptome sequencing reveals thousands of novel long non-coding RNAs in B cell lymphoma. *Genome Med*. 2015;7(1):110.
13. Iqbal J, Shen Y, Huang X, et al. Global microRNA expression profiling uncovers molecular markers for classification and prognosis in aggressive B-cell lymphoma. *Blood*. 2015;125(7):1137-1145.
14. Musilova K, Mraz M. MicroRNAs in B-cell lymphomas: how a complex biology gets more complex. *Leukemia*. 2015;29(5):1004-1017.
15. Bartel DP. MicroRNAs: genomics, biogenesis, mechanism, and function. *Cell*. 2004;116(2):281-297.
16. Blower PE, Chung J-H, Verducci JS, et al. MicroRNAs modulate the chemosensitivity of tumor cells. *Mol Cancer Ther*. 2008;7(1):1-9.
17. Marques SC, Ranjbar B, Laursen MB, et al. High miR-34a expression improves response to doxorubicin in diffuse large B-cell lymphoma. *Exp Hematol*. 2016;44(4):238-246.
18. Rasmussen MH, Lyskjær I, Jersie-Christensen RR, et al. miR-625-3p regulates oxaliplatin resistance by targeting MAP2K6-p38 signalling in human colorectal adenocarcinoma cells. *Nat Commun*. 2016;7(1):12436.

## Acknowledgments

The authors greatly appreciate the technical assistance from Louise Hvilshøj Madsen and Helle Høholt, Department of Hematology, Aalborg University Hospital, Aalborg, Denmark.

This study was supported by grants from The Danish Cancer Society and The North Region Research Foundation, Denmark.

## Authorship

Contribution: H.D., A.S.R., and K.D. designed the research; H.D., M.X., X.T., Y.P., K.E.Y., and K.D. collected the data; H.D., L.R., M.N.P., D.S.J., and E.A.T. performed experiments; H.D., J.G.M., and K.D. optimized the experimental setup; H.D., A.A.S., and M.B. performed statistical analysis and generated the figures; H.D. wrote the paper; and all authors contributed to data interpretation and critically revised and approved the final manuscript.

Conflict-of-interest disclosure: The authors declare no competing financial interests.

Correspondence: Karen Dybkær, Department of Clinical Medicine/Aalborg University and Department of Hematology, Aalborg University Hospital, Sdr Skovvej 15, 9000 Aalborg, Denmark; e-mail: k.dybkaer@rn.dk.

19. Due H, Svendsen P, Bødker JS, et al. miR-155 as a biomarker in B-Cell malignancies. *BioMed Res Int*. 2016;2016:9513037.
20. Kluiver J, Kroesen B-J, Poppema S, van den Berg A. The role of microRNAs in normal hematopoiesis and hematopoietic malignancies. *Leukemia*. 2006; 20(11):1931-1936.
21. Jardin F, Figeac M. MicroRNAs in lymphoma, from diagnosis to targeted therapy. *Curr Opin Oncol*. 2013;25(5):480-486.
22. Babar IA, Cheng CJ, Booth CJ, et al. Nanoparticle-based therapy in an in vivo microRNA-155 (miR-155)-dependent mouse model of lymphoma. *Proc Natl Acad Sci USA*. 2012;109(26):E1695-E1704.
23. Falgreen S, Dybkær K, Young KH, et al. Predicting response to multidrug regimens in cancer patients using cell line experiments and regularised regression models. *BMC Cancer*. 2015;15(1):235.
24. Lenz G, Wright G, Dave SS, et al; Lymphoma/Leukemia Molecular Profiling Project. Stromal gene signatures in large-B-cell lymphomas. *N Engl J Med*. 2008;359(22):2313-2323.
25. Falgreen S, Laursen MB, Bødker JS, et al. Exposure time independent summary statistics for assessment of drug dependent cell line growth inhibition. *BMC Bioinformatics*. 2014;15(1):168.
26. Dybkær K, Bøgsted M, Falgreen S, et al. Diffuse large B-cell lymphoma classification system that associates normal B-cell subset phenotypes with prognosis. *J Clin Oncol*. 2015;33(12):1379-1388.
27. Ranjbar B, Krogh LB, Laursen MB, et al. Anti-apoptotic effects of lentiviral vector transduction promote increased rituximab tolerance in cancerous B-cells. *PLoS One*. 2016;11(4):e0153069.
28. Rasmussen TK, Andersen T, Bak RO, et al. Overexpression of microRNA-155 increases IL-21 mediated STAT3 signaling and IL-21 production in systemic lupus erythematosus. *Arthritis Res Ther*. 2015;17(1):154.
29. Bak RO, Hollensen AK, Primo MN, Sørensen CD, Mikkelsen JG. Potent microRNA suppression by RNA Pol II-transcribed 'Tough Decoy' inhibitors. *RNA*. 2013;19(2):280-293.
30. Hollensen AK, Thomsen R, Bak RO, et al. Improved microRNA suppression by WPRE-linked tough decoy microRNA sponges. *RNA*. 2017;23(8): 1247-1258.
31. Sanjana NE, Shalem O, Zhang F. Improved vectors and genome-wide libraries for CRISPR screening. *Nat Methods*. 2014;11(8):783-784.
32. Brinkman EK, Chen T, Amendola M, van Steensel B. Easy quantitative assessment of genome editing by sequence trace decomposition. *Nucleic Acids Res*. 2014;42(22):e168.
33. R Core Team. R: A Language and Environment for Statistical Computing. Vienna, Austria: R Foundation for Statistical Computing; 2017.
34. Irizarry RA, Hobbs B, Collin F, et al. Exploration, normalization, and summaries of high density oligonucleotide array probe level data. *Biostatistics*. 2003; 4(2):249-264.
35. Ritchie ME, Phipson B, Wu D, et al. limma powers differential expression analyses for RNA-sequencing and microarray studies. *Nucleic Acids Res*. 2015; 43(7):e47.
36. Johnson WE, Li C, Rabinovic A. Adjusting batch effects in microarray expression data using empirical Bayes methods. *Biostatistics*. 2007;8(1):118-127.
37. Leek JT, Johnson WE, Parker HS, Jaffe AE, Storey JD. The sva package for removing batch effects and other unwanted variation in high-throughput experiments. *Bioinformatics*. 2012;28(6):882-883.
38. Subramanian A, Tamayo P, Mootha VK, et al. Gene set enrichment analysis: a knowledge-based approach for interpreting genome-wide expression profiles. *Proc Natl Acad Sci USA*. 2005;102(43):15545-15550.
39. Liberzon A, Birger C, Thorvaldsdóttir H, Ghandi M, Mesirov JP, Tamayo P. The Molecular Signatures Database (MSigDB) hallmark gene set collection. *Cell Syst*. 2015;1(6):417-425.
40. Butz H, Likó I, Czirják S, et al. Down-regulation of Wee1 kinase by a specific subset of microRNA in human sporadic pituitary adenomas. *J Clin Endocrinol Metab*. 2010;95(10):E181-E191.
41. Tili E, Michaille J-J, Wernicke D, et al. Mutator activity induced by microRNA-155 (miR-155) links inflammation and cancer. *Proc Natl Acad Sci USA*. 2011;108(12):4908-4913.
42. Visconti R, Della Monica R, Palazzo L, et al. The Fcp1-Wee1-Cdk1 axis affects spindle assembly checkpoint robustness and sensitivity to antimicrotubule cancer drugs. *Cell Death Differ*. 2015;22(9):1551-1560.
43. Cheson BD, Pfistner B, Juweid ME, et al; International Harmonization Project on Lymphoma. Revised response criteria for malignant lymphoma. *J Clin Oncol*. 2007;25(5):579-586.
44. Ma X, Becker Buscaglia LE, Barker JR, Li Y. MicroRNAs in NF-kappaB signaling. *J Mol Cell Biol*. 2011;3(3):159-166.
45. Davis RE, Brown KD, Siebenlist U, Staudt LM. Constitutive nuclear factor kappaB activity is required for survival of activated B cell-like diffuse large B cell lymphoma cells. *J Exp Med*. 2001;194(12):1861-1874.
46. Clark PM, Loher P, Quann K, Brody J, Londin ER, Rigoutsos I. Argonaute CLIP-Seq reveals miRNA targetome diversity across tissue types. *Sci Rep*. 2014;4(1):5947.
47. Musacchio A, Salmon ED. The spindle-assembly checkpoint in space and time. *Nat Rev Mol Cell Biol*. 2007;8(5):379-393.
48. Gascoigne KE, Taylor SS. Cancer cells display profound intra- and interline variation following prolonged exposure to antimitotic drugs. *Cancer Cell*. 2008;14(2):111-122.
49. Rieder CL, Maiato H. Stuck in division or passing through: what happens when cells cannot satisfy the spindle assembly checkpoint. *Dev Cell*. 2004;7(5): 637-651.

50. Ghelli Luserna Di Rora A, Iacobucci I, Beeharry N, et al. The Wee1 inhibitor, MK-1775, sensitizes leukemic cells to different antineoplastic drugs interfering with DNA damage response pathway. *Blood*. 2015;126(23):1276.
51. Hirai H, Arai T, Okada M, et al. MK-1775, a small molecule Wee1 inhibitor, enhances anti-tumor efficacy of various DNA-damaging agents, including 5-fluorouracil. *Cancer Biol Ther*. 2010;9(7):514-522.
52. Huang X, Shen Y, Liu M, et al. Quantitative proteomics reveals that miR-155 regulates the PI3K-AKT pathway in diffuse large B-cell lymphoma. *Am J Pathol*. 2012;181(1):26-33.
53. Costinean S, Sandhu SK, Pedersen IM, et al. Src homology 2 domain-containing inositol-5-phosphatase and CCAAT enhancer-binding protein beta are targeted by miR-155 in B cells of Emicro-MiR-155 transgenic mice. *Blood*. 2009;114(7):1374-1382.
54. Lee E-R, Kim J-Y, Kang Y-J, et al. Interplay between PI3K/Akt and MAPK signaling pathways in DNA-damaging drug-induced apoptosis. *Biochim Biophys Acta*. 2006;1763(9):958-968.
55. Doublier S, Riganti C, Voena C, et al. RhoA silencing reverts the resistance to doxorubicin in human colon cancer cells. *Mol Cancer Res*. 2008;6(10):1607-1620.
56. Pouliot LM, Chen Y-C, Bai J, et al. Cisplatin sensitivity mediated by WEE1 and CHK1 is mediated by miR-155 and the miR-15 family. *Cancer Res*. 2012;72(22):5945-5955.
57. Lv L, An X, Li H, Ma L. Effect of miR-155 knockdown on the reversal of doxorubicin resistance in human lung cancer A549/dox cells. *Oncol Lett*. 2016;11(2):1161-1166.
58. Pallasch CP, Leskov I, Braun CJ, et al. Sensitizing protective tumor microenvironments to antibody-mediated therapy. *Cell*. 2014;156(3):590-602.
59. Zhong H, Xu L, Zhong J-H, et al. Clinical and prognostic significance of miR-155 and miR-146a expression levels in formalin-fixed/paraffin-embedded tissue of patients with diffuse large B-cell lymphoma. *Exp Ther Med*. 2012;3(5):763-770.
60. Go H, Jang J-Y, Kim P-J, et al. MicroRNA-21 plays an oncogenic role by targeting FOXO1 and activating the PI3K/AKT pathway in diffuse large B-cell lymphoma. *Oncotarget*. 2015;6(17):15035-15049.